

## Mirror Mode Waves at Comet Halley

C. T. Russell and Guan Le  
Institute of Geophysics and Planetary Physics University of California,  
Los Angeles, CA 90024-1567

K. Schwingenschuh and W. Riedler, Space Research Institute, Graz, Austria

Ye. Yeroshenko, IZMIRAN, Moscow Region, USSR

**Abstract.** High resolution VEGA magnetic field and plasma data in Halley's magnetosphere reveal out-of-phase oscillations of the type expected to be driven by the mirror mode instability. The spacecraft passes through these structures in about 20 s. The magnetic energy density drops about  $6.5 \times 10^9$  ergs/cm<sup>3</sup> in a typical event. The thickness of these regions is about a water-group ion gyro diameter. While such enhancements should be invisible against the comet when viewed perpendicular to the wavefronts, they could be visible as rays when viewed tangential to the wavefronts.

### Introduction

On their closest approach to Halley on March 6 and 9, 1986 the VEGA spacecraft detected numerous small-scale depressions in the magnetic field [Yeroshenko et al., 1986]. The magnetometer included a fourth sensor to measure gradients in the field [Riedler et al., 1986] but no gradients were observed in these events indicating they were large-scale phenomena occurring within the ambient medium and not on the spacecraft itself [Yeroshenko et al., 1987]. These events were first postulated to be associated with critical ionization velocity effects [Galeev et al., 1986]. However, Trotignon et al. [1989] have shown that the plasma waves that were taken to be diagnostic of the CIV process are more likely due to dust impacts. An alternate explanation of these small-scale depressions, proposed by Russell et al. [1987], was that these events were in fact the magnetic signature of the mirror mode instability. This mechanism would account for the increases in ion density observed in conjunction with the magnetic decreases on VEGA-1 [Vaisberg et al., 1989] and VEGA-2 [Russell et al., 1987].

The analyses of these waves to date have been rather brief. The properties of these waves have

not been completely described, nor have all the waves been analyzed. It is the purpose of this paper both to compile what we know about these structures and to complete the analysis of these waves. We begin with the VEGA-2 data which contain the fewer events.

### Observations

Only one axis of the VEGA-2 magnetometer survived closest approach, thus we can analyze the fluctuations over only the inbound portion of the trajectory. Figure 1 shows the magnetic field

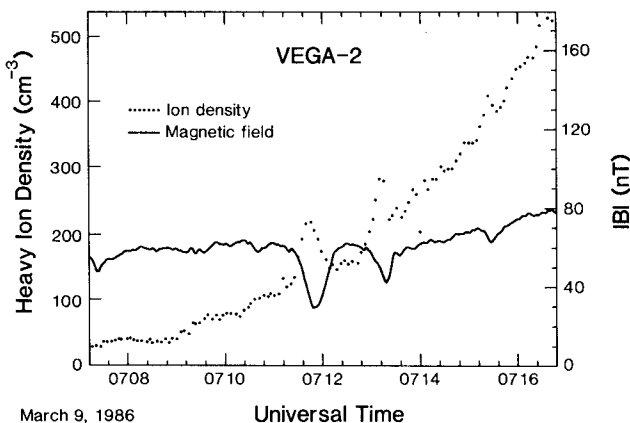


Fig. 1. The magnitude of the magnetic field and the ion density measured on the inbound leg of VEGA-2 from 0708 to 0716 UT, March 9, 1986 [Galeev et al., 1986; Gringauz et al., 1986; Riedler et al., 1986].

strength and the ion density measured by the PLASMAG-1 detector [Gringauz et al., 1986]. There are three dips in the magnetic field, centered at 0711:48, 0713:20, and 0715:31 UT. Each dip has a corresponding increase in the plasma density. The dips last about 20 s and are separated in time by

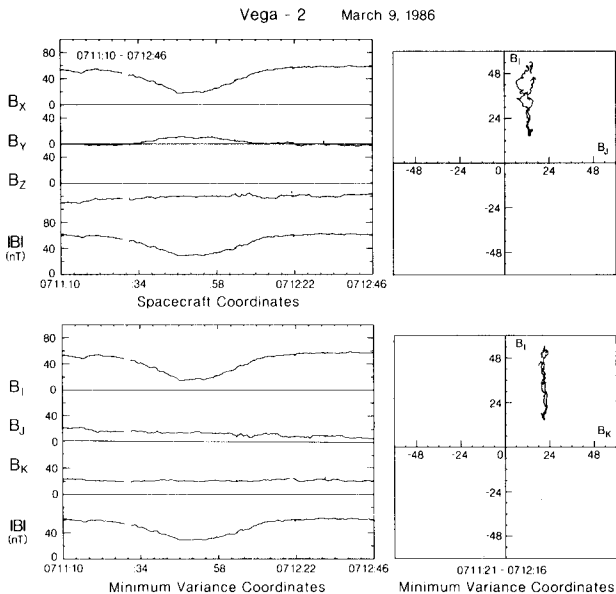


Fig. 2. High resolution measurements (10/second) of the magnetic field measured by VEGA-2 from 0711:10 to 0712:46 on March 9, 1986 at a distance of 40,000 km from the nucleus of comet Halley. The top left panel shows the data in spacecraft coordinates roughly oriented along the solar ecliptic axes. The bottom left panel shows the data rotated to the minimum variance or principal axis system. The right-hand panels show hodograms of the magnetic field as the disturbance is crossed [Russell et al., 1987].

a period greater than their duration. Figure 2 shows high resolution, 0.1 sec, measurements across the first of these fluctuations. The fluctuation is shown as a time series both in spacecraft coordinates and in principal axis coordinates, and in the form of hodograms in principal axis coordinates.

The principal axis data show that the variation occurs along a single direction in the plasma but that this direction is not parallel to the magnetic field. There is a significant non-field-aligned component of the fluctuation. The fluctuation is therefore not a simple diamagnetic depression, i.e., a non-propagating disturbance in pressure equilibrium, but rather it appears to be a slow mode wave propagating at an oblique angle to the magnetic field. We can find the direction of propagation by noting that the direction of the field perturbation must be perpendicular to the direction of propagation as should the vector cross product of the background magnetic field and the field change. Thus the triple cross product of first the background magnetic field times the field change and then times the field change again gives the direction of propagation. We defer an analysis of the direction of propagation to a later section of this paper. Table 1 lists the location of each

of these events, the background field, the field change, the duration of the event and the change in magnetic energy during the event. All vectors are given in comet-centered solar-ecliptic coordinates with x directed toward the sun, and z along the ecliptic pole. The background magnetic field is an average of the field before and after the event. The change in field is the difference in the field at the center of the depression and this background field. The duration of the event is taken to be the period over which the field depression is greater than 50% of its maximum depression. The change in magnetic energy density is the difference between the magnetic energy measured at the peak of the event and the average of the before and after energy densities.

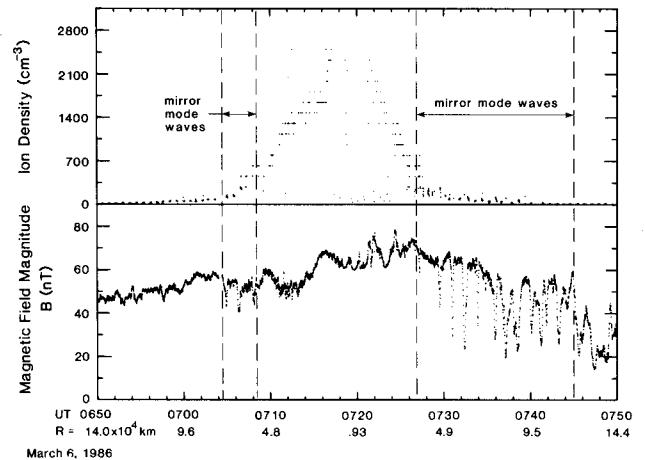


Fig. 3. (Top). Time series of heavy ion number densities measured within the hour of closest approach to comet Halley by the BD-3 plasma detector on VEGA-1. (Bottom). Simultaneously measured of the strength of the magnetic field [Vaisberg et al., 1989].

Figure 3 shows the time series of heavy ion densities measured during the hour of closest approach to VEGA-1 together with the simultaneously measured magnetic field magnitude [Vaisberg et al., 1989]. Inbound at about 70,000 km from the nucleus are 3 fluctuations similar to those seen inbound along the VEGA-2 trajectory. Outbound there are even more of these waves. Again the events are narrow compared to their separation with few exceptions. We first examine the 3 events inbound which occurred roughly in the same location as the VEGA-2 events described above.

Table 1 lists the observed properties of the events. The background field strength is a little weaker during the VEGA-1 inbound events (50 nT versus 60 nT) because these events are observed further from the nucleus than on VEGA-2. The change in field for each of the events is weaker than the 2 larger VEGA-2 events but larger than the weakest VEGA-2 event. The duration of the events is also similar at about 20 s.

Table 1. Observed Properties of Events

| Time           | Background B           | Change in B         | Location                           | Duration | $\Delta(B^2/8\pi)$           |
|----------------|------------------------|---------------------|------------------------------------|----------|------------------------------|
| 0704:54 Day 65 | (-30.1, 35.0, 20.3) nT | (-6.0, 4.5, 10.1)   | (-1.8, 7.0, -0.6) $\times 10^4$ km | 15 s     | $4.7 \times 10^{-9}$ ergs/cc |
| 0706:19        | (-23.6, 34.3, 26.7)    | (-8.1, 8.9, 3.3)    | (-1.6, 6.3, -0.6)                  | 26       | 5.1                          |
| 0708:06        | (-22.9, 32.5, 33.2)    | (-3.7, 5.6, 8.2)    | (-1.2, 5.6, -0.5)                  | 21       | 3.2                          |
| 0726:40        | (25.7, 64.0, 0.1)      | (1.1, 3.5, 5.5)     | (1.9, -2.5, 0.6) $\times 10^4$ km  | 9        | 2.9                          |
| 0727:12        | (23.0, 57.7, 19.4)     | (7.7, 9.2, -1.8)    | (2.0, -2.8, 0.7)                   | 5        | 5.3                          |
| 0729:31        | (22.0, 53.2, 20.0)     | (6.3, 17.6, -8.4)   | (2.4, -3.8, 0.8)                   | 12       | 9.0                          |
| 0730:59        | (24.9, 55.0, -1.0)     | (24.2, 31.6, 2.7)   | (2.7, -4.4, 0.9)                   | 9        | 12.1                         |
| 0732:22        | (25.0, 55.8, 5.3)      | (26.6, 33.4, 12.8)  | (2.9, -5.0, 1.0)                   | 24       | 13.6                         |
| 0733:54        | (23.8, 52.0, 21.7)     | (22.3, 21.7, 16.4)  | (3.2, -5.7, 1.1)                   | 7        | 11.4                         |
| 0734:47        | (16.6, 40.4, 34.6)     | (1.4, 3.9, 9.3)     | (3.3, -6.1, 1.1)                   | 5        | 3.7                          |
| 0735:53        | (12.7, 32.5, 31.6)     | (9.9, 15.3, 19.9)   | (3.5, -6.6, 1.2)                   | 13       | 6.6                          |
| 0736:30        | (14.4, 37.9, 33.0)     | (6.7, 7.3, 1.3)     | (3.6, -6.8, 1.2)                   | 8        | 2.9                          |
| 0736:50        | (15.4, 38.7, 31.4)     | (6.4, 8.0, 13.9)    | (3.7, -7.0, 1.2)                   | 10       | 7.6                          |
| 0737:05        | (8.1, 29.3, 24.9)      | (0.7, 13.3, 18.2)   | (3.7, -7.1, 1.2)                   | 16       | 5.2                          |
| 0737:48        | (14.2, 26.4, 37.4)     | (2.0, 9.2, -0.8)    | (3.8, -7.4, 1.3)                   | 3        | 2.4                          |
| 0738:27        | (17.9, 41.5, 23.6)     | (10.3, 16.7, 29.2)  | (3.9, -7.7, 1.3)                   | 17       | 9.1                          |
| 0740:04        | (16.6, 42.4, 23.8)     | (9.2, 15.7, 12.6)   | (4.2, -8.4, 1.4)                   | 21       | 7.8                          |
| 0741:13        | (14.6, 41.0, 10.5)     | (8.8, 19.3, 11.0)   | (4.4, -8.9, 1.5)                   | 20       | 6.3                          |
| 0741:51        | (9.4, 42.8, 16.9)      | (7.7, 17.0, 6.3)    | (4.5, -9.2, 1.5)                   | 9        | 5.4                          |
| 0742:32        | (14.6, 47.1, 20.3)     | (0.2, 5.6, 4.5)     | (4.6, -9.5, 1.5)                   | 9        | 3.3                          |
| 0743:14        | (9.7, 41.8, 22.0)      | (7.1, 17.5, 16.1)   | (4.8, -9.8, 1.6)                   | 22       | 7.4                          |
| 0711:48 Day 68 | (45.2, -21.3, -15.4)   | (33.0, -20.0, -0.9) | (-0.8, 3.8, -0.3)                  | 28       | 8.3                          |
| 0713:20        | (47.3, -18.8, -4.6)    | (17.5, -10.5, 1.5)  | (-0.5, 3.1, -0.2)                  | 16       | 7.7                          |
| 0715:31        | (55.6, -26.2, -1.9)    | (5.1, -3.0, 3.0)    | (-0.1, 2.2, -0.1)                  | 9        | 4.2                          |

As can be seen from Figure 3 there appear to be many more events outbound than inbound. The events occur over a greater range of radial distance and are deeper. Otherwise the fluctuations are very similar to those seen inbound. Figure 4 shows an example of the outbound fluctuations at 0733:55 UT. It is quite a smoothly varying feature, almost linearly polarized. Figure 5 shows a second example at a greater radial distance. The hodograms look similar to the earlier events except that the depressions last longer in time. This tendency is also evident in Figure 3.

The 24 events listed in Table 1 provide a good statistical sample of this phenomenon. The average event lasts 14 seconds, and during the event the magnetic energy density decreases  $6.5 \times 10^{-9}$  ergs/cm<sup>3</sup>. They are found out to radial distances of  $7 \times 10^4$  km when VEGA was behind the nucleus to over  $10^5$  km in front. There is a range of distances near the nucleus over which the events are not seen. Reference to Figure 3 shows that this is the region over which the ion density was greater than about 1000 cm<sup>-3</sup>.

Figure 6 shows the locations of the events seen along the two trajectories. The top panels show projections of the two trajectories in cometary solar ecliptic coordinates. The VEGA-2 trace has only an inbound leg. The panels on the left show the view from above the solar ecliptic and on the right the view from the Sun. The bottom panels show the trajectory rotated to keep the magnetic field in the Y-direction. Symmetry has been invoked to double the coverage in the left-hand panel by assuming no right-left asymmetry and to quadruple the coverage in the right-hand panel by assuming 4-fold symmetry, east-west and north-south. From the available coverage there seems to be no preference in occurrence location except to occur within  $10^5$  km of the nucleus.

#### Derived Properties of the Events

As noted above it is possible to derive the direction of propagation of these fluctuations from the triple cross product of the background magnetic field, the field change and the field change again

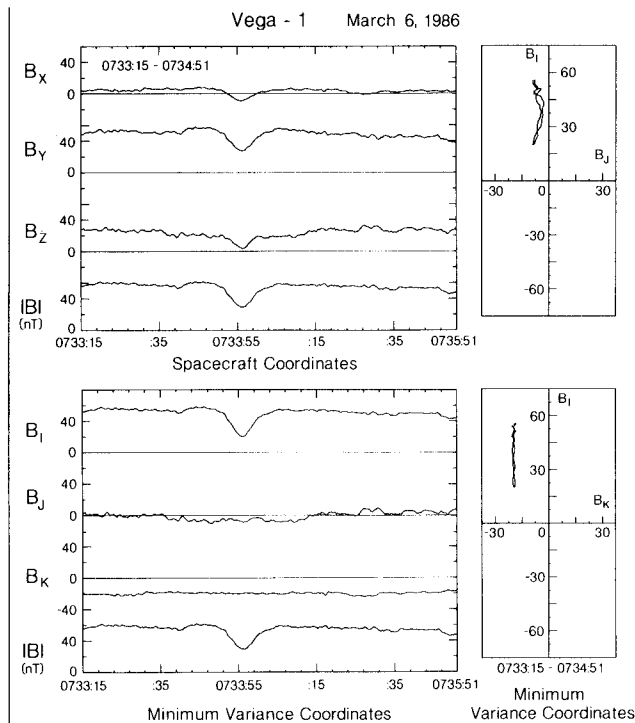


Fig. 4. High resolution measurements of the magnetic field from 0733:15 to 0735:51 UT on March 6, 1986 during the VEGA-1 encounter with comet Halley. See caption of Figure 2 for further details.

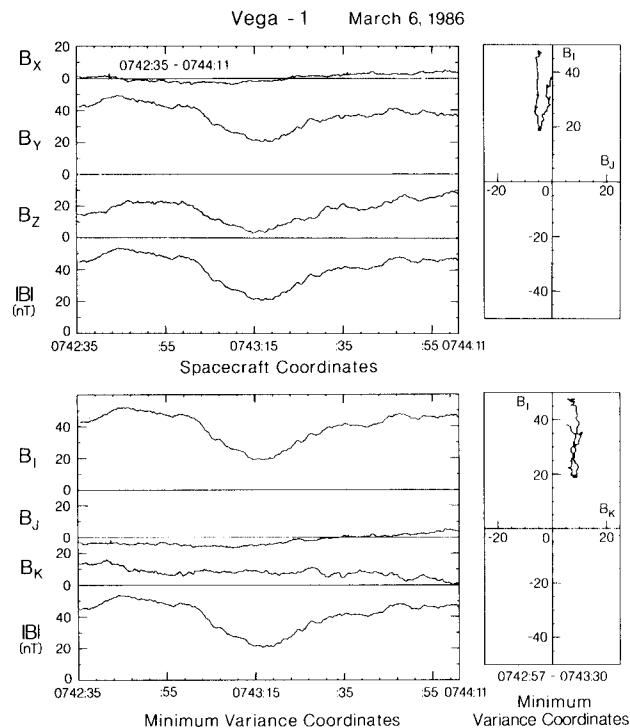


Fig. 5. High resolution measurements of the magnetic field from 0742:35 to 0744:11 UT on March 6, 1986 during the VEGA-1 encounter with comet Halley. See caption of Figure 2 for further details.

under the assumption that these features are magnetosonic waves. Since these fluctuations have a strong anticorrelation between the number density and the field strength and since the hodograms of the waves reveal a wave-like rather than discontinuity like structure we feel this is an accurate assumption. Table 2 lists the direction of propagation for those fluctuations for which we believe the background magnetic field remains sufficiently steady during the event and the event was sufficiently strong ( $> 10$  nT). This amounts to about only 1/3 of the events. The average direction of propagation to the field is  $72^\circ$  with a slight tendency for the direction of propagation to be more perpendicular to the field at greater distances from the nucleus.

To the extent the plasma is at rest and the wave velocity much lower than the speed of the VEGA spacecraft relative to Halley we can calculate the velocity of the spacecraft perpendicular to the wavefronts and convert the event durations into sizes. The average thickness is 800 km. Although most of the events have thicknesses close to the average, we note that 2 do not. This suggests that despite our caution in analyzing steady events some non-steady fields were included.

### Plasma Properties

As shown in Figures 1 and 3 there is an anti-correlation between the magnetic field and the plasma density in these events. This anti-correlation has been treated in detail by Vaisberg et al. [1989] using the VEGA-1 measurements of the BD-3 plasma detector. This correlation is shown in Figure 7 for all events for which the BD-3 detector was operating in its sensitive mode. Figure 7 extends beyond the end of the period for which we believe we can accurately analyze the direction of propagation of the events. In fact there is only one event in Figure 7 that we believe is steady enough and deep enough to analyze in detail with some confidence. That is event number 2.

However, we can use the anti-correlation between the field strength and plasma density to derive an ion temperature under the assumption that the sum of the magnetic and ion pressures is constant across the events. This is done in Figure 8 and the results summarized in Figure 9 and Table 3. Figure 8 also shows a model ion temperature which demonstrates that the ion temperatures obtained are generally as expected with the possible difference

Table 2. Derived Properties of Events

| Time            | $\underline{k}$    | $\theta_{Bk}$ | $V_{11}$ | $D_{50z}$ |
|-----------------|--------------------|---------------|----------|-----------|
| 0704:54 Day 065 | (-.37, .75, -.55)  | 59°           | 71 km/s  | 1060 km   |
| 0729:31         | (-.25, -.34, -.91) | 61°           | 9        | 110       |
| 0730:59         | (-.77, 0.60, -.20) | 76°           | 67       | 600       |
| 0733:54         | (-.57, 0.78, -.25) | 68°           | 76       | 530       |
| 0735:53         | (-.42, 0.80, -.43) | 77°           | 75       | 970       |
| 0741:13         | (0.08, 0.47, -.88) | 75°           | 41       | 810       |
| 0741:51         | (-.82, 0.47, -.30) | 83°           | 61       | 550       |
| 0743:14         | (-.05, 0.69, -.73) | 76°           | 73       | 1610      |
| 0711:48 Day 068 | (0.16, 0.31, -.94) | 73°           | 27       | 760       |

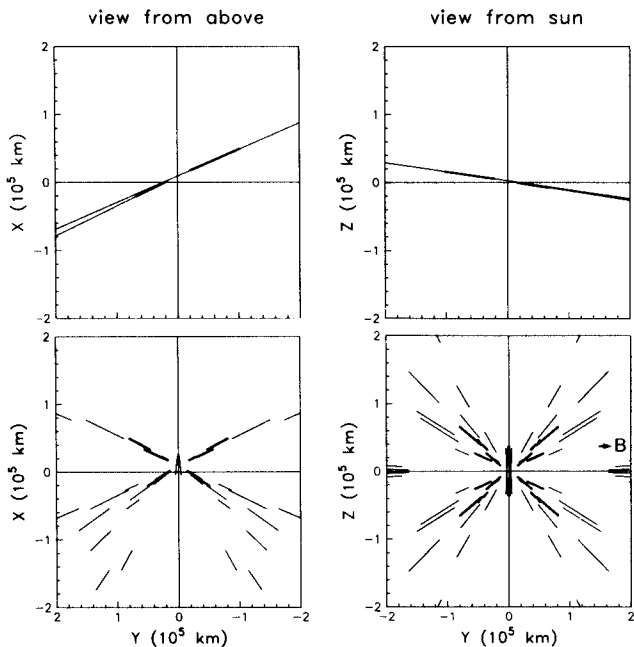


Fig. 6. The trajectory of VEGA-1 and -2 past comet Halley showing with a heavy line the location of the apparent mirror mode fluctuations. The top 2 panels show the projections as seen from above the ecliptic plane (left) and from the sun (right). The bottom 2 panels show the location in a coordinate system that keeps the magnetic field in the Y-direction. The left-hand panel assumes left-right symmetry of wave occurrence. The right-hand panel assumes left-right symmetry as well as top-bottom symmetry in occurrence.

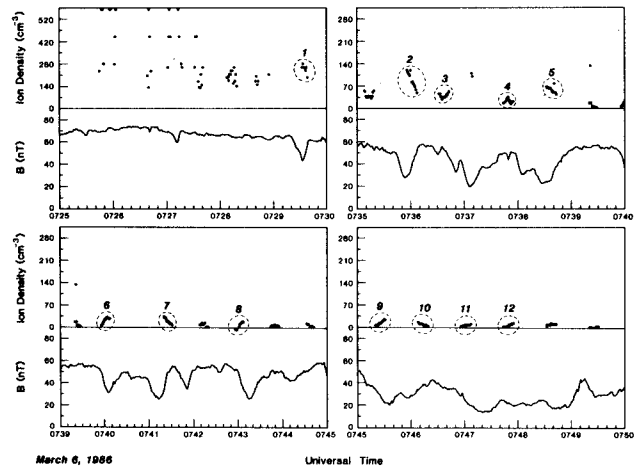


Fig. 7. Magnifications of sections of Figure 3 showing the detailed anti-correlation of the field strength and plasma density [Vaisberg et al., 1989].

that they are colder near the nucleus and warmer further from the nucleus than the model predicts.

Table 3 also displays the water group ion gyro radius for the 6 events of the 12 for which we have some confidence in our measurement of duration, ion temperature and density. The gyro radius is about 450 km. Thus these structures have a thickness of about an ion gyro diameter, if the relative velocity of the structures and the spacecraft is dominated by the spacecraft velocity relative to the nucleus. We note that the one event in which we have some confidence, the 0735:53 UT event, agrees with our statistical comparison.

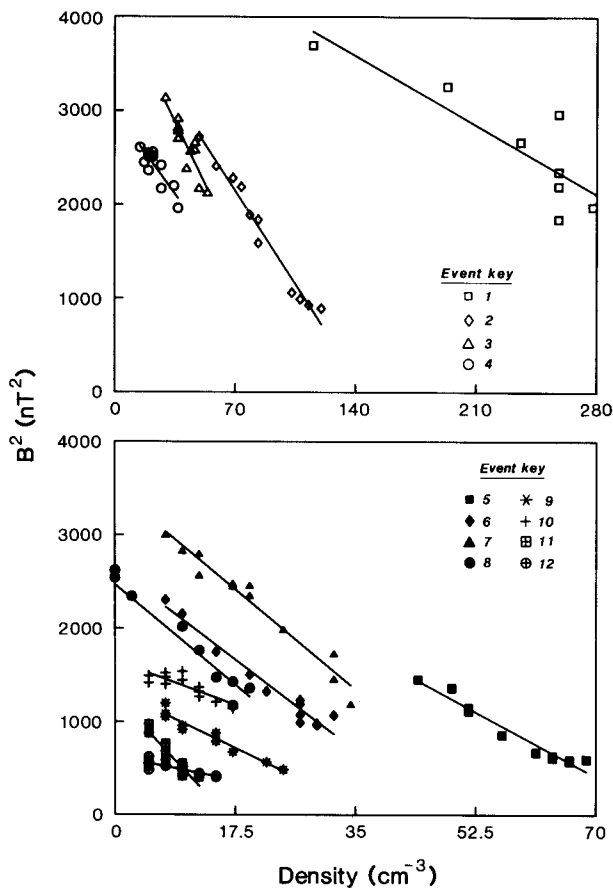


Fig. 8. Plots of the magnetic field squared versus density obtained from each of the structures numbered in Figure 7. Lines show least square fits to the data [Vaisberg et al., 1989].

Discussion

The fluctuations discussed above seem at first unusual. They are quite different from the waves seen at larger distances and which appear to be fast magnetosonic waves (e.g., Smith et al., 1986). Rather, these waves have the characteristics of slow magnetosonic waves. Such waves are not unknown in space plasmas. Figure 10 shows a series of fluctuations observed by ISEE-2 just outside the magnetopause. These magnetosheath waves have been shown by Crooker et al. [1977] and by Moustazis et al. [1986] to have the properties of slow mode waves perhaps driven by the mirror instability. The major difference is that in the magnetosheath the field depressions last a time equal or longer than the enhancements, whereas in the cometary magnetosphere the field depressions are relatively brief. Figure 11 shows an analysis of a typical magnetosheath slow or mirror mode fluctuation presented in the format of Figures 2, 4 and 5. This shows that the form of the fluctuation is

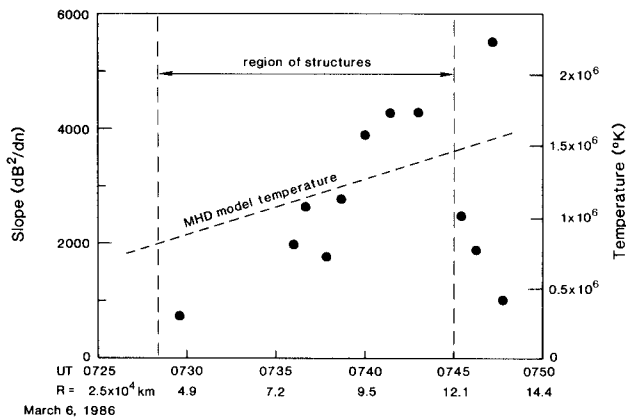


Fig. 9. The slopes of the segments shown in Figure 8 as well as their conversion to ion temperature. Plasma temperatures from an MHD model are also shown for comparison [Vaisberg et al., 1989].

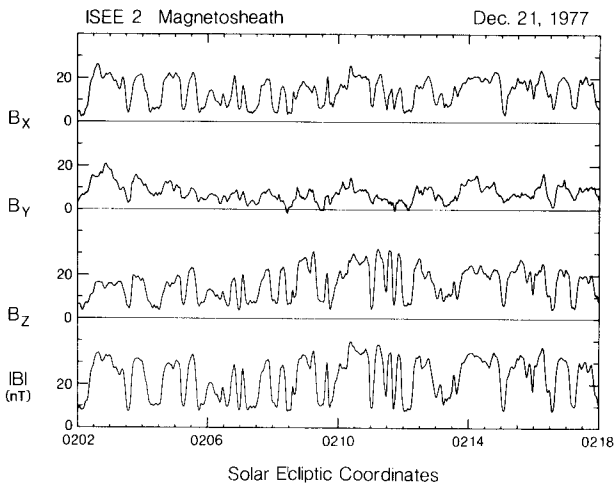


Fig. 10. ISEE-2 magnetic field measurements in solar ecliptic coordinates in the magnetosheath just outside the magnetopause during an interval of mirror-mode like waves.

indeed very similar. Figure 12 shows another example. This one is from a disturbance deep in interplanetary space [Russell, 1990]. Thus, this form of disturbance occurs under a wide range of conditions.

We have stated above that such waves have the properties of slow mode or mirror mode waves. Figure 13 illustrates the structure of such a wave [Siscoe, 1983]. The sinusoids represent the magnetic field lines. The dashed lines show wavefronts propagating at a large angle to the magnetic field. The ions occupy the weak field region, mirroring between the stronger fields to the top and bottom of the diagram. The observed thickness of these structures of about one ion gyro diameter is consistent with this picture.

Table 3. Plasma Properties of Events

| Time    | $M_{max}$     | $T_i$             | $B_{ext}$ | $R_g^{WG}$ | $D_{50\%}$ |
|---------|---------------|-------------------|-----------|------------|------------|
| 0729:31 | 280 $cm^{-3}$ | $3 \times 10^5$ K | 61        | 217        | (110)      |
| 0735:53 | 120           | 8                 | 47        | 460        | 970        |
| 0736:30 | 60            | 11                | 52        | 487        | ---        |
| 0737:48 | 40            | 7                 | 48        | 421        | ---        |
| 0738:27 | 70            | 12                | 51        | 520        | (809)      |
| 0740:04 | 33            | 16                | 51        | 600        | (720)      |

Note: ( ) = less confidence in data.

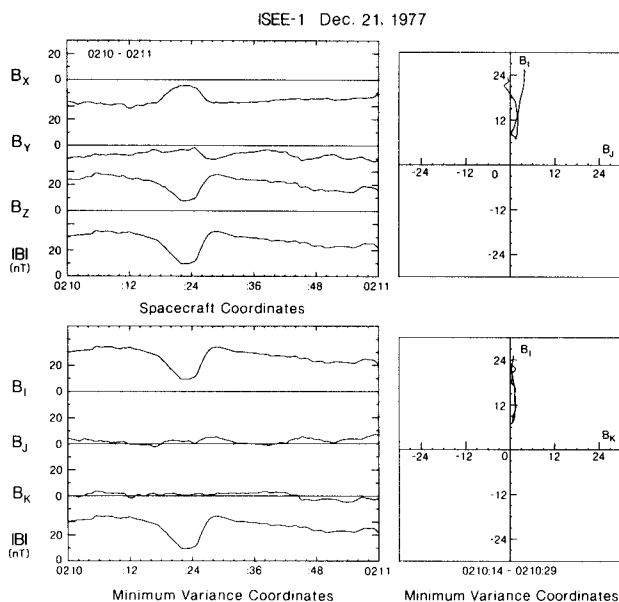


Fig. 11. ISEE-1 magnetosheath measurements analyzed in a manner similar to that used in Figures 2, 4 and 5.

Under normal circumstances, however, this instability is not expected to be the most unstable. Rather the ion cyclotron instability which is also driven by a greater perpendicular than parallel temperature should have the higher growth rate. This is illustrated in Figure 14 which shows the growth rate of various plasma modes under typical plasma conditions [Barnes, 1979]. Perhaps the answer lies in the multicomponent nature of the plasma which will modify the growth rate of the ion cyclotron waves [Price et al., 1986]. It is unfortunate that we do not have measurements of the temperature anisotropies so

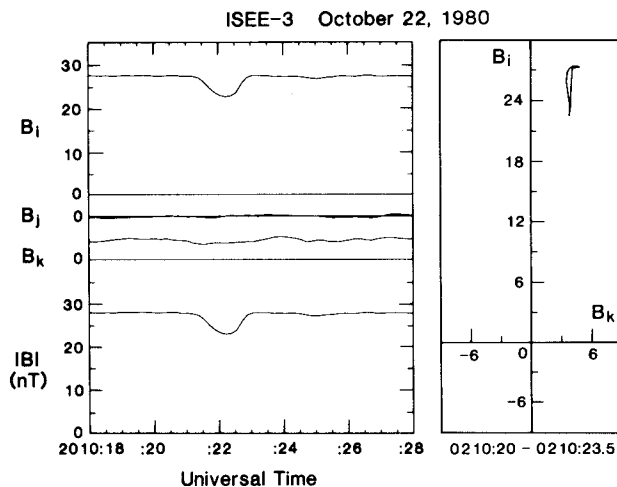


Fig. 12. ISEE-3 magnetic field measurements of a fluctuation deep in interplanetary space which appears also to be a mirror-mode oscillation [Russell, 1989].

that we could determine if the mirror mode was in fact unstable.

An important question is whether such structures which clearly have ray like properties are in fact the cause of visible cometary rays. We note that the density enhancement in these structures drops with distance from the nucleus as the ion temperatures rise. Thus these structures will have the greatest effect closer to the nucleus. On the other hand, they disappear on both VEGA 1 and 2 close to the nucleus. If we take our largest enhancement of  $280 \text{ cm}^{-3}$  and a 220 km ion gyro radius we obtain an enhancement integrated along the line-of-sight of  $10^9 \text{ ion/cm}^3$  if our line-of-sight is perpendicular to the plane containing the ions. We would not see this against the background of the comet which contains at least 1000 times

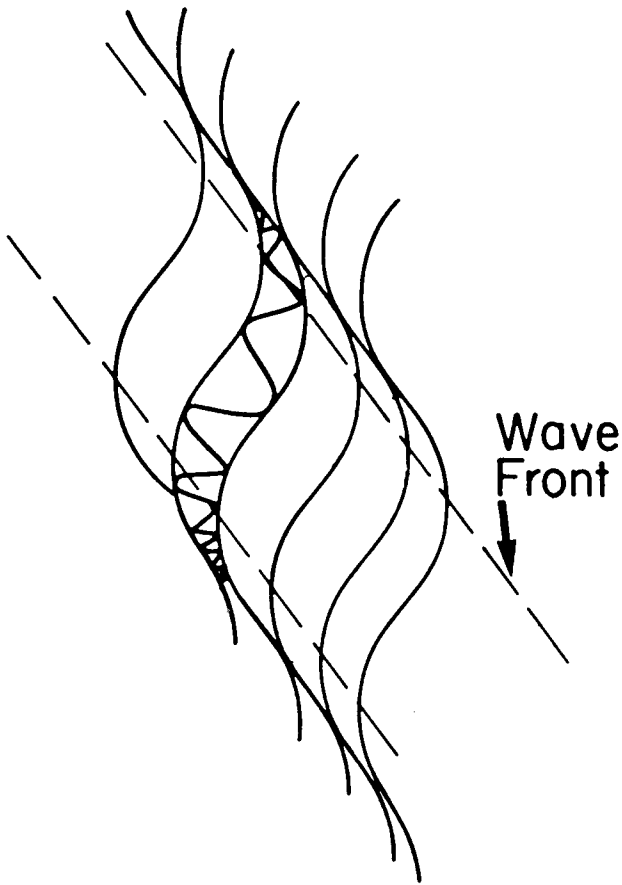


Fig. 13. The relationship between the field line oscillations (sinusoids), the wavefronts and the ion motion in a mirror-mode wave [Siscoe, 1983].

this integrated density [Russell et al., 1989]. However, if one were to look tangent to the wavefront, one might get a sufficient enhancement in visual emissions. Moreover, the enhancement would have more of the appearance of a ray under such geometry than if viewed perpendicular to the wavefront.

#### Conclusions

The VEGA 1 and 2 magnetometers and ion instruments detected fluctuations in the magnetic field and ion density that appear to be slow mode or mirror mode waves. These waves are propagating at a large angle to the magnetic field and have scale sizes of approximately a gyro diameter. They may be responsible for condensing ions into structures that become visible when observed edge on.

**Acknowledgments.** This research was supported by the National Aeronautics and Space Administration under research grant NAGW-717.

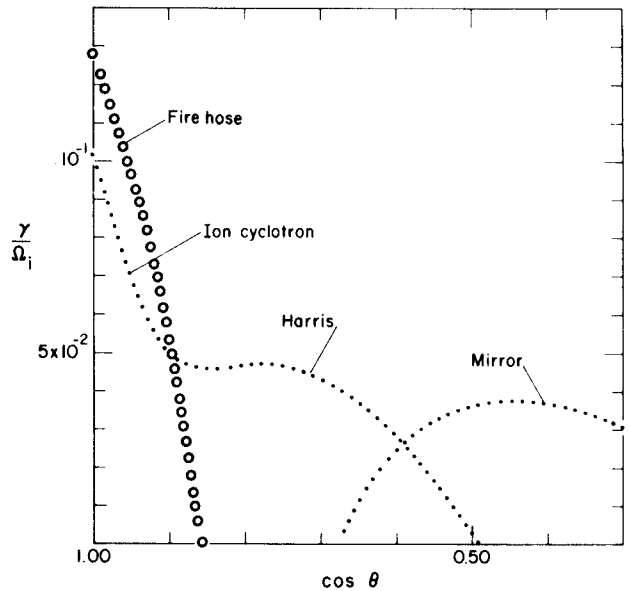


Fig. 14. The growth rate of various plasma instabilities for typical plasma conditions as a function of the direction of the propagation vector relative to the magnetic field [Barnes, 1979].

#### References

- Barnes, A., Hydromagnetic waves and turbulence in the solar wind, in *Solar System Plasma Physics*, (eds. E. N. Parker, C. F. Kennel and L. J. Lanzerotti), North Holland Publ. Co., 1979.
- Crooker, N. U. and G. L. Siscoe, A mechanism for pressure anisotropy and mirror instability in the dayside magnetosheath, *J. Geophys. Res.*, **82**, 185, 1977.
- Galeev, A. A., et al., Critical ionization velocity effects in the inner coma of comet Halley: Measurements by VEGA-2 *Geophys. Res. Lett.*, **13**, 845-848, 1986.
- Gringauz, K. I., et al., First in-situ plasma and neutral gas measurements at comet Halley, *Nature*, **321**, 282-285, 1986.
- Moustaizis, S., et al., Magnetohydrodynamic turbulence in the earth's magnetosheath, *Ann. Geophys.*, **4**, 355-362, 1986.
- Price, C. P., D. W. Swift and L. C. Lee, Numerical simulation of nonoscillatory mirror waves at the earth's magnetosheath, *J. Geophys. Res.*, **91**, 101-112, 1986.
- Riedler, W., K. Schwingenschuh, Ye. G. Yeroshenko, V. A. Styashkin and C. T. Russell, Magnetic field observations in comet Halley's coma, *Nature*, **321**, 288-289, 1986.
- Russell, C. T., Interplanetary magnetic field enhancements: Evidence for solar wind dust trail interactions, *Adv. Space Res.*, **10**, (3)159- (3)162, 1990.

